

## Octupole-deformed molecular bands in $^{21}\text{Ne}$

Wheldon, Carl; Kokalova, Tzanka; von Oertzen, W

DOI:

[10.1140/epja/i2005-10186-y](https://doi.org/10.1140/epja/i2005-10186-y)

### Document Version

Publisher's PDF, also known as Version of record

### Citation for published version (Harvard):

Wheldon, C, Kokalova, T & von Oertzen, W 2006, 'Octupole-deformed molecular bands in  $^{21}\text{Ne}$ ', *European Physical Journal A*, vol. 26, no. 3, pp. 321-326. <https://doi.org/10.1140/epja/i2005-10186-y>

[Link to publication on Research at Birmingham portal](#)

### General rights

Unless a licence is specified above, all rights (including copyright and moral rights) in this document are retained by the authors and/or the copyright holders. The express permission of the copyright holder must be obtained for any use of this material other than for purposes permitted by law.

- Users may freely distribute the URL that is used to identify this publication.
- Users may download and/or print one copy of the publication from the University of Birmingham research portal for the purpose of private study or non-commercial research.
- User may use extracts from the document in line with the concept of 'fair dealing' under the Copyright, Designs and Patents Act 1988 (?)
- Users may not further distribute the material nor use it for the purposes of commercial gain.

Where a licence is displayed above, please note the terms and conditions of the licence govern your use of this document.

When citing, please reference the published version.

### Take down policy

While the University of Birmingham exercises care and attention in making items available there are rare occasions when an item has been uploaded in error or has been deemed to be commercially or otherwise sensitive.

If you believe that this is the case for this document, please contact [UBIRA@lists.bham.ac.uk](mailto:UBIRA@lists.bham.ac.uk) providing details and we will remove access to the work immediately and investigate.

# Octupole-deformed molecular bands in $^{21}\text{Ne}$

C. Wheldon<sup>1,a</sup>, Tz. Kokalova<sup>1,2</sup>, W. von Oertzen<sup>1,2</sup>, S. Thummerer<sup>1</sup>, H.G. Bohlen<sup>1</sup>, B. Gebauer<sup>1</sup>, A. Tumino<sup>1</sup>, T.N. Massey<sup>3</sup>, G. de Angelis<sup>4</sup>, M. Axiotis<sup>4</sup>, A. Gadea<sup>4</sup>, Th. Kröll<sup>4</sup>, N. Mărginean<sup>4</sup>, D.R. Napoli<sup>4</sup>, M. De Poli<sup>4</sup>, C. Ur<sup>4</sup>, D. Bazzacco<sup>5</sup>, S.M. Lenzi<sup>5</sup>, C. Rossi Alvarez<sup>5</sup>, S. Lunardi<sup>5</sup>, R. Menegazzo<sup>5</sup>, P.G. Bizzeti<sup>6</sup>, and A.M. Bizzeti-Sona<sup>6</sup>

<sup>1</sup> SF7, Hahn-Meitner-Institut, Glienicke Straße 100, D-14109 Berlin, Germany

<sup>2</sup> Fachbereich Physik, Freie Universität Berlin, Arnimallee 14, D-14195 Berlin, Germany

<sup>3</sup> Department of Physics and Astronomy, Ohio University, Athens, OH, USA

<sup>4</sup> INFN, Laboratori Nazionali di Legnaro, Via Romea 4, I-35020 Legnaro (Padova), Italy

<sup>5</sup> Dipartimento di Fisica dell'Università and INFN, Sezione di Padova, I-35131 Padova, Italy

<sup>6</sup> Dipartimento di Fisica dell'Università and INFN, Via G. Sansone 1, I-50019 Sesto Fiorentino (Firenze), Italy

Received: 18 October 2005 / Revised version: 30 November 2005 /

Published online: 11 January 2006 – © Società Italiana di Fisica / Springer-Verlag 2006

Communicated by R. Krücken

**Abstract.** Cluster states up to 12 MeV in the stable light nucleus  $^{21}\text{Ne}$ , based on the  $^{16}\text{O} + n + \alpha$  molecular configurations, have been populated in the incomplete-fusion reaction  $^{16}\text{O}(^7_3\text{Li}, n p)^{21}_{10}\text{Ne}$  at 29.4 MeV. The observation of both intra- and inter-band transitions leads to a re-interpretation of some levels in the  $K^\pi = \frac{3}{2}^-$  and  $K^\pi = \frac{1}{2}^-$  bands. The implications of this re-ordering on the octupole doublet bands are examined. The data allow a more accurate determination of some previously uncertain level energies. The “missing”  $I^\pi = \frac{5}{2}^-$  level is also discussed.

**PACS.** 23.20.Lv  $\gamma$  transitions and level energies – 25.70.Hi Transfer reactions – 27.30.+t  $20 \leq A \leq 38$

## 1 Introduction

Structures exhibited by many light nuclei can be described by underlying tightly bound cores, clustered together into molecular-like systems. For example, the ground states of some beryllium nuclei ( $Z = 4$ ) can be described by two  $\alpha$ -particle cores [1,2]. Experimentally, such shapes give rise to rotational bands, often with extremely large moments of inertia [3]. For some neon isotopes ( $Z = 10$ ), evidence has been reported for structures comprising  $\alpha$ -particle and  $^{16}\text{O}$  sub-clusters [4]. The size difference between these two species necessarily leads to a reflection asymmetric nuclear potential, a characteristic of which is the formation of parity-doublet rotational bands [4]. In  $^{20}\text{Ne}$ , for example, two bands with  $K^\pi = 0^\pm$  are observed [3,4], where  $K$  is the projection of the total angular momentum onto the nuclear symmetry axis. The addition of a neutron to this system maintains the reflection asymmetric shape and leads to the formation of two parity-inversion bands in  $^{21}\text{Ne}$ , namely the  $K^\pi = \frac{3}{2}^+$  ground-state band and its  $K^\pi = \frac{3}{2}^-$  partner band and the  $K^\pi = \frac{1}{2}^\pm$  configuration. Neon-21 is particularly good for investigating this phenomenon because, although three of the four octupole

bands are far from yrast, they lie predominantly below the particle thresholds, in contrast to  $^{20}\text{Ne}$ , and have non-negligible intraband  $\gamma$ -ray decay branches. The neutron and  $\alpha$ -particle thresholds lie at 6.761 and 7.348 MeV, respectively, compared to the cluster bandheads which all lie below 3.7 MeV.

Here we report new results on the octupole doublet bands in  $^{21}\text{Ne}$  obtained with the GASP+ISIS setup.

## 2 Experimental method

Cluster states up to 12 MeV in  $^{21}\text{Ne}$  have been populated in the incomplete-fusion reaction  $^{16}\text{O}(^7_3\text{Li}, n p)^{21}_{10}\text{Ne}$ . The “oxygen” target consisted of 600  $\mu\text{g}/\text{cm}^2$  beryllium oxide, enriched to 94% in  $^{10}\text{Be}$ , backed firstly by 4.9  $\text{mg}/\text{cm}^2$  platinum and secondly by 40  $\text{mg}/\text{cm}^2$  gold. The 29.4 MeV DC  $^7\text{Li}$  beam was provided by the XTU-Tandem at Legnaro National Laboratory. The GASP spectrometer [5], comprising forty Compton-suppressed co-axial germanium detectors, was used in conjunction with the ISIS charged-particle detector [6]. The geometry of ISIS is such that one  $\Delta E$ - $E$  silicon telescope sits in front of each germanium detector. The master trigger required a good event in the ISIS charged-particle detector and two germanium detectors to fire. Energy and efficiency calibrations

<sup>a</sup> e-mail: wheldon@hmi.de;

URL: <http://www.hmi.de/people/wheldon/>.

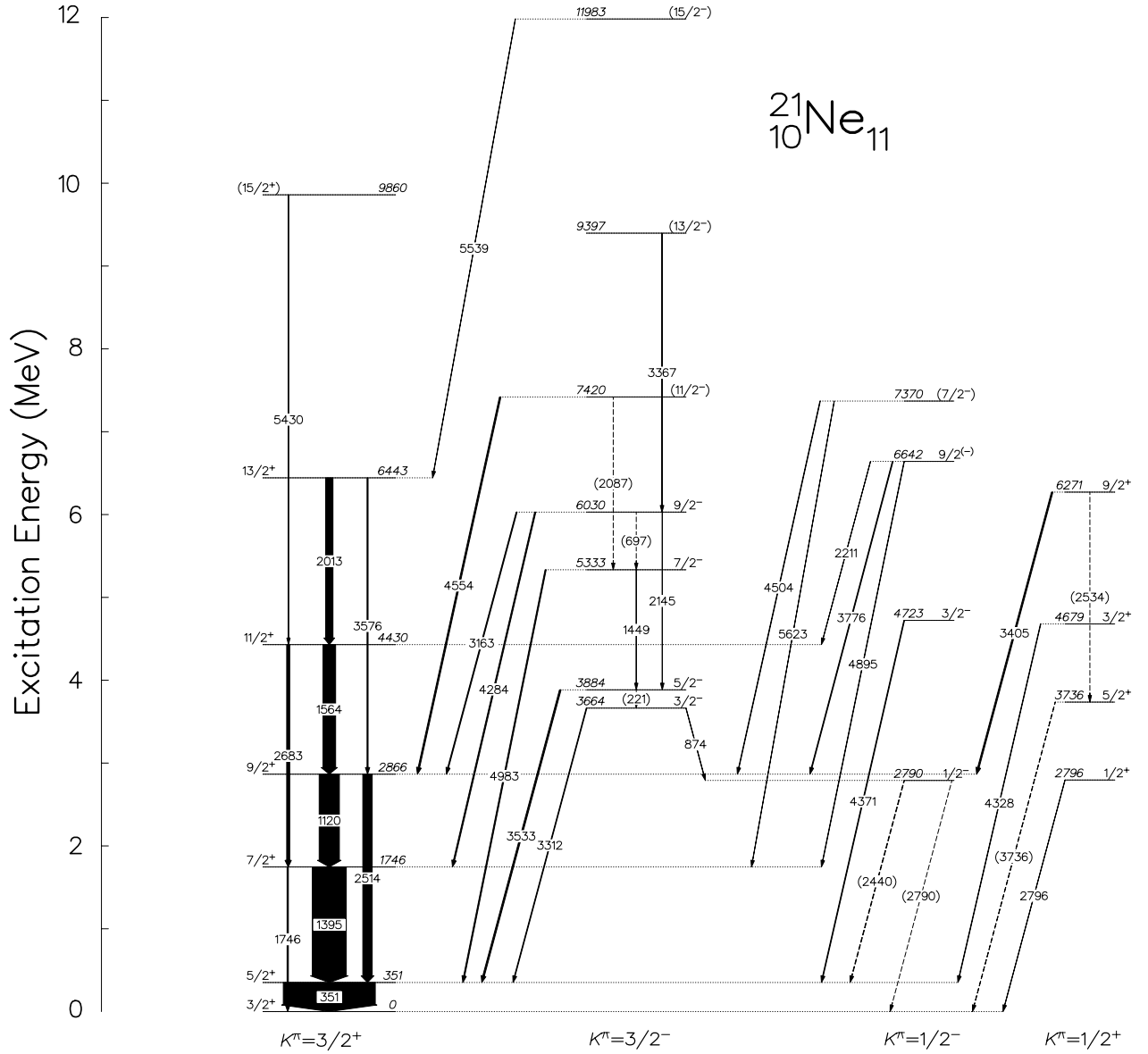


**Fig. 1.** Partial level scheme for the cluster bands in  $^{21}\text{Ne}$  observed in the current work. The widths of the arrows are proportional to intensity. Tentatively observed transitions are indicated by dashed arrows. The spin and parity assignments are taken from refs. [11, 9].

for the germanium detectors were obtained using  $^{56}\text{Co}$  and  $^{152}\text{Eu}$  sources. Note that the highest energy calibration point lies at 3451 keV, and  $\gamma$ -ray transitions exceeding this energy therefore rely on extrapolating the energy and efficiency calibration curves, increasing the uncertainties.

Doppler-corrected, particle-gated 1- and 2-dimensional histograms were produced using the GASPWARE sorting program [7] and analysed using the RADWARE software package [8]. Gamma- $\gamma$  coincidence matrices gated by protons detected in ISIS have been constructed to enable the study of  $^{21}\text{Ne}$ , by far the most intense neon isotope. In fig. 1, the partial level scheme for the cluster bands obtained in the current work is shown. Table 1 gives detailed information, with uncertainties quoted where relevant.

Part of the data presented here have been reported in ref. [9]. However, a reanalysis of these data using the background subtraction method published in ref. [10] has resulted in significant differences to ref. [9] (predominantly additional transitions have been identified), allowing the cluster bands to be rearranged and discussed in more detail.

### 3 Results

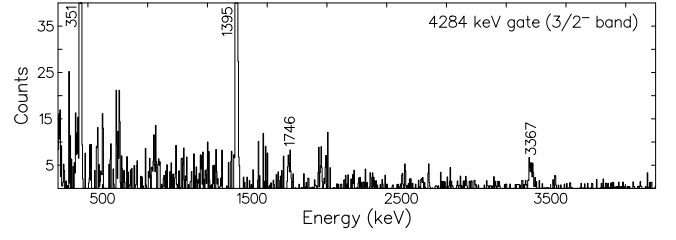
#### 3.1 The $\frac{3}{2}^{+}$ (ground-state) band

The yrast, ground-state band with a  $K^{\pi} = \frac{3}{2}^{+}$  assignment [11], is observed up to the  $I^{\pi} = (\frac{15}{2}^{+})$  state at

**Table 1.** Energies, assignments and relative intensities for transitions observed in  $^{21}\text{Ne}$ .

$E_\gamma$ (keV)	$I_\gamma$ (arb.)	$E_i$ (keV)	$E_f$ (keV)	$I_i^\pi, K_i$ ( $\hbar$ )	$I_f^\pi, K_f$ ( $\hbar$ )
(221)	weak	3884.2(4)	3664	$\frac{5}{2}^-, \frac{3}{2}$	$\frac{3}{2}^-, \frac{3}{2}$
351.2(2)	370(20)	351.2(1)	0	$\frac{5}{2}^-, \frac{3}{2}$	$\frac{3}{2}^-, \frac{3}{2}$
(697)	weak	6029.6(4)	5333	$\frac{5}{2}^-, \frac{3}{2}$	$\frac{3}{2}^-, \frac{3}{2}$
873.7(8)	1.10(8)	3663.7(5)	2790	$\frac{5}{2}^-, \frac{3}{2}$	$\frac{1}{2}^-, \frac{1}{2}$
1120.2(2)	81.2(25)	2865.9(2)	1746	$\frac{5}{2}^-, \frac{3}{2}$	$\frac{5}{2}^-, \frac{3}{2}$
1394.7(2)	137(4)	1745.8(2)	351	$\frac{5}{2}^-, \frac{3}{2}$	$\frac{5}{2}^-, \frac{3}{2}$
1448.7(15)	0.16(6)	5333.4(6)	3884	$\frac{5}{2}^-, \frac{3}{2}$	$\frac{5}{2}^-, \frac{3}{2}$
1564.0(2)	51.0(16)	4429.8(2)	2866	$\frac{11}{2}^+, \frac{3}{2}$	$\frac{5}{2}^-, \frac{3}{2}$
1746.1(8)	5.2(3)	1745.8(2)	0	$\frac{5}{2}^-, \frac{3}{2}$	$\frac{5}{2}^-, \frac{3}{2}$
2013.5(2)	29.5(9)	6443.3(3)	4430	$\frac{13}{2}^+, \frac{3}{2}$	$\frac{11}{2}^+, \frac{3}{2}$
(2087)	weak	7419.8(6)	5333	$(\frac{11}{2}^-), \frac{3}{2}$	$\frac{7}{2}^-, \frac{3}{2}$
2145.1(12)	1.09(8)	6029.6(4)	3884	$\frac{9}{2}^-, \frac{1}{2}$	$\frac{5}{2}^-, \frac{3}{2}$
2211.0(15)	0.58(8)	6641.5(6)	4430	$\frac{9}{2}^-, \frac{1}{2}$	$\frac{11}{2}^+, \frac{3}{2}$
(2440)	weak	2790.3(5)	351	$\frac{5}{2}^-, \frac{3}{2}$	$\frac{5}{2}^-, \frac{3}{2}$
2514.0(5)	37.9(12)	2865.9(2)	351	$\frac{5}{2}^-, \frac{3}{2}$	$\frac{5}{2}^-, \frac{3}{2}$
(2534)	weak	6270.8(5)	3736	$\frac{5}{2}^-, \frac{3}{2}$	$\frac{5}{2}^-, \frac{3}{2}$
2683.3(7)	12.1(4)	4429.8(2)	1746	$\frac{11}{2}^+, \frac{3}{2}$	$\frac{5}{2}^-, \frac{3}{2}$
(2790)	weak	2790.3(5)	0	$\frac{5}{2}^-, \frac{3}{2}$	$\frac{5}{2}^-, \frac{3}{2}$
2795.5(22)	0.9(14)	2795.5(15)	0	$\frac{5}{2}^-, \frac{3}{2}$	$\frac{5}{2}^-, \frac{3}{2}$
3163.5(7)	3.51(14)	6029.6(4)	2866	$\frac{5}{2}^-, \frac{3}{2}$	$\frac{5}{2}^-, \frac{3}{2}$
3311.8(12)	2.69(16)	3663.7(5)	351	$\frac{5}{2}^-, \frac{3}{2}$	$\frac{5}{2}^-, \frac{3}{2}$
3367.3(19)	1.26(10)	9396.9(13)	6030	$(\frac{13}{2}^-), \frac{3}{2}$	$\frac{5}{2}^-, \frac{3}{2}$
3405.0(7)	5.74(24)	6270.8(5)	2866	$\frac{9}{2}^-, \frac{1}{2}$	$\frac{5}{2}^-, \frac{3}{2}$
3532.9(7)	6.3(3)	3884.2(4)	351	$\frac{5}{2}^-, \frac{3}{2}$	$\frac{5}{2}^-, \frac{3}{2}$
3575.6(13)	4.11(19)	6443.3(3)	2866	$\frac{13}{2}^+, \frac{3}{2}$	$\frac{5}{2}^-, \frac{3}{2}$
(3736)	weak	3736.0(14)	0	$\frac{5}{2}^-, \frac{3}{2}$	$\frac{5}{2}^-, \frac{3}{2}$
3776.2(10)	2.98(14)	6641.5(6)	2866	$\frac{9}{2}^-, \frac{1}{2}$	$\frac{5}{2}^-, \frac{3}{2}$
4284.4(9)	4.66(18)	6029.6(4)	1746	$\frac{9}{2}^-, \frac{1}{2}$	$\frac{5}{2}^-, \frac{3}{2}$
4328(3)	1.65(18)	4679.3(22)	351	$\frac{5}{2}^-, \frac{3}{2}$	$\frac{5}{2}^-, \frac{3}{2}$
4371.4(15)	2.74(16)	4722.6(10)	351	$\frac{5}{2}^-, \frac{3}{2}$	$\frac{5}{2}^-, \frac{3}{2}$
4504.3(18)	1.79(11)	7369.9(11)	2866	$(\frac{7}{2}^-), \frac{1}{2}$	$\frac{5}{2}^-, \frac{3}{2}$
4553.8(9)	5.93(22)	7419.8(6)	2866	$(\frac{11}{2}^-), \frac{3}{2}$	$\frac{5}{2}^-, \frac{3}{2}$
4895.0(22)	1.42(10)	6641.5(6)	1746	$\frac{9}{2}^-, \frac{1}{2}$	$\frac{7}{2}^+, \frac{3}{2}$
4982.7(11)	4.30(21)	5333.4(6)	351	$\frac{7}{2}^-, \frac{3}{2}$	$\frac{5}{2}^-, \frac{3}{2}$
5430(4)	0.47(8)	9859.8(25)	4430	$(\frac{15}{2}^+), \frac{3}{2}$	$\frac{11}{2}^+, \frac{3}{2}$
5539.3(21)	0.90(7)	11982.5(14)	6443	$(\frac{15}{2}^-), \frac{3}{2}$	$\frac{13}{2}^+, \frac{3}{2}$
5623(4)	0.58(7)	7369.9(11)	1746	$(\frac{7}{2}^-), \frac{1}{2}$	$\frac{7}{2}^+, \frac{3}{2}$

9860 keV. The transitions up to the 6443 keV level are well known [11], but the 5430 keV decay has not previously been reported, though the 9860 keV state is known from Hoffman *et al.* [12] at 9867 keV and Hallock *et al.* [13] at 9840(15) keV. The excitation energy of 9859.8(25) keV obtained here is in agreement with the compiled value of 9857(1) keV [11]. Note that the 9860 keV level had two possible placements in previous work [3,9], but here is placed as the  $I^\pi = (\frac{15}{2}^+)$  level in the ground-state band.

**Fig. 2.** Gamma-ray spectrum gated by the 4284 keV transition from the lowest  $\frac{3}{2}^-$  band. The 3367 keV in-band decay can be clearly seen. Labelled peaks are assigned to  $^{21}\text{Ne}$ .

### 3.2 The $\frac{3}{2}^-$ band at 3664 keV

The structure built on the  $K^\pi = \frac{3}{2}^-$  state at 3664 keV has been observed up to  $I^\pi = (\frac{15}{2}^-)$  in this work. In-band transitions,  $(\frac{13}{2}^-) \rightarrow \frac{9}{2}^-$ ,  $\frac{9}{2}^- \rightarrow \frac{5}{2}^-$  and  $\frac{7}{2}^- \rightarrow \frac{5}{2}^-$  have been firmly established (see fig. 2). In addition to the in-band transitions, intense out-of-band decays to the  $K^\pi = \frac{3}{2}^+$  band are identified for all but the  $(\frac{13}{2}^-)$ , 9397 keV band member. The latter decay is known [12], though too weak to observe here.

The  $I = \frac{9}{2}$  and  $(\frac{11}{2})$  rotational levels of this band at 6030 and 7420 keV, respectively, as shown in fig. 1, differ from those that appear in the literature [3,9]. For the  $\frac{9}{2}$  state this follows from the clear observation of in-band transitions both to (3367 keV) and from (2145 keV) the 6030 keV level. Such transitions were not observed for the earlier assigned 6641 keV state. For the 7420 keV ( $\frac{11}{2}$ ) level, tentative evidence for a 2087 keV in-band decay to the  $\frac{7}{2}$  member of the band, together with the non-observation of the earlier assigned 7960 keV level, favours the current placement. (The earlier reported 5093 keV (7960 keV  $\rightarrow$  2866 keV)  $\gamma$  ray in ref. [9] is actually the 5111 keV transition (not shown in fig. 1) from a state at 7976 keV to the same final level (2866 keV).) The new placement of the 7420 keV level favours the  $I^\pi = \frac{11}{2}^-$  assignment rather than the alternative  $I^\pi = \frac{7}{2}^+$  label [11]. This state has been observed at 7413(10) by Hallock *et al.* [13] using the  $^{13}\text{C}(^{12}\text{C}, \alpha)$  reaction, at 7424 keV by Andritsopoulos *et al.* [14] using the  $^{12}\text{C}(^{13}\text{C}, \alpha \gamma)$  reaction, at 7426(5) keV by Rolfs *et al.* [15] and at 7422 keV by Hoffman *et al.* [12], both using the  $^{18}\text{O}(\alpha, n \gamma)$  reaction. In the latter both the out-of-band decay to the 2866 keV level and the weak in-band decay to the 5333 keV level were reported as well as the 3367 keV  $(\frac{13}{2}^-) \rightarrow \frac{9}{2}^-$  transition, which becomes an in-band decay in the newly arranged scheme. The energy of the  $(\frac{11}{2}^-)$  level was determined here to be 7419.8(6) keV, in close agreement with earlier work and the 7422.8(7) keV compiled value [11].

### 3.3 The $\frac{1}{2}^+$ band at 2796 keV

The levels in the  $K^\pi = \frac{1}{2}^+$  band have been observed here up to the  $I^\pi = \frac{9}{2}^+$  member, with states as proposed for

this band in refs. [3,9]. No in-band transitions have been firmly identified, though there is tentative evidence for a  $\Delta I = 2$ , 2534 keV decay between the  $\frac{9}{2}^+$  and  $\frac{5}{2}^+$  levels. Earlier work by Hoffmann *et al.* [12] reported weak out-of-band decays from the  $\frac{9}{2}^+$  state to the 4430, 1746 and 351 keV states in the  $K^\pi = \frac{3}{2}^+$  ground-state band, in addition to the strong transition to the 2866 keV member, which is observed here. Instead, here a 2534 keV in-band  $\gamma$  ray has been tentatively observed which has not previously been identified. The decays to the 351 and 1746 keV states could not be confirmed here due to other, close-lying transitions. Previous studies that observed states in this band include refs. [15,16], ref. [13] (though not the 4679 keV  $I^\pi = \frac{3}{2}^+$  level) and Grawe *et al.* [17] (apart from the 6271 keV level), using the  $^2\text{H}(^{20}\text{Ne}, p\gamma)$  reaction. One other in-band transition has previously been reported between the  $\frac{3}{2}^+$  and  $\frac{1}{2}^+$  levels [18], but this was not confirmed by Andritsopoulos *et al.* [14]. Finally, the centroid energy of the 4679.3(22) keV state reported here is  $\approx 5$  keV lower than the compiled value of 4684.56(15) keV [11]. A possible explanation is the large number of transitions around 4328 keV, at which the only transition de-exciting this  $\frac{3}{2}^+$  level was observed.

### 3.4 The $\frac{1}{2}^-$ band at 2790 keV

Here, states at 2790 ( $\frac{1}{2}^-$ ), 4723 ( $\frac{3}{2}^-$ ), 6642 ( $\frac{5}{2}^-$ ) and 7370 keV ( $\frac{7}{2}^-$ ) are observed. The 6642 keV state has been newly placed in this band, following the identification of the previously assigned 6030 keV state as a member of the  $K^\pi = \frac{3}{2}^-$  band (sect. 3.2).

The level energy of 7369.9(11) keV is above the centroid of the compiled value at 7357(14) keV [11] which has previously eluded precise determination. Rolfs *et al.* [15] measured a similar value (7375(5) keV) and Andritsopoulos *et al.* [14] obtained 7363(15) keV, with other studies reporting 7360(10) keV [13] and 7363(15) keV [12].

### 3.5 Other bands

In addition to the four cluster bands described above, three deformed bands have been proposed [3], based on the Nilsson orbitals,  $\nu: \{\frac{1}{2}^+[220]\}$  ( $K^\pi = \frac{1}{2}^+$ ),  $\{\frac{3}{2}^+[211]\}$  ( $K^\pi = \frac{3}{2}^+$ ) and  $\{\frac{5}{2}^+[202]\}$  ( $K^\pi = \frac{5}{2}^+$ ). The energies, which differ from those in ref. [3] because of new assignments to the cluster bands, are given in table 2.

## 4 Discussion

The  $K = \frac{3}{2}$  and  $\frac{1}{2}$  parity-doublet bands have been interpreted [3,9] as arising from an underlying cluster structure formed by  $^{16}\text{O} + n + \alpha$ . The rearrangement of some of the levels between the four bands, as described in sect. 3, strengthens this interpretation. Figure 3 shows the excitation energies of all of the rotational bands. The spacing of

**Table 2.** Levels proposed for the three normal-deformed Nilsson bands in  $^{21}\text{Ne}$ . Energies in italics indicate levels with tentative assignments. The energies of the states, when observed in the present work, are given underneath, in small, bold font and with accompanying parentheses where tentatively identified.

$I^\pi$	$K^\pi = \frac{1}{2}^+$	$K^\pi = \frac{3}{2}^+$	$K^\pi = \frac{5}{2}^+$
( $\hbar$ )	(keV)		
$\frac{1}{2}^+$	5690 <sup>(a)</sup>		
	<b>5690</b>		
$\frac{3}{2}^+$	5821	5550 ( $\approx 5551$ )	
$\frac{5}{2}^+$	<i>6175</i> <b>6169</b>	<i>5774</i>	4526 <b>4526</b>
$\frac{7}{2}^+$	6412 <sup>(b)</sup>	<i>6260</i> <b>6257</b>	<i>5432</i> <b>5428</b>
$\frac{9}{2}^+$	<i>7042</i> <b>7042</b>		<i>6544</i> <b>6538</b>
$\frac{11}{2}^+$	<i>8241</i> <b>8237</b>		<i>7982</i> <b>7977</b>
$\frac{13}{2}^+$			<i>9700</i> <sup>(c)</sup> ( $\approx 9690$ )

(a) Change of parity with respect to the compilation [11].

(b) No current assignment in ref. [11].

(c) Based on tentative evidence of a newly observed  $\approx 5260$  keV decay to the 4430 keV state.

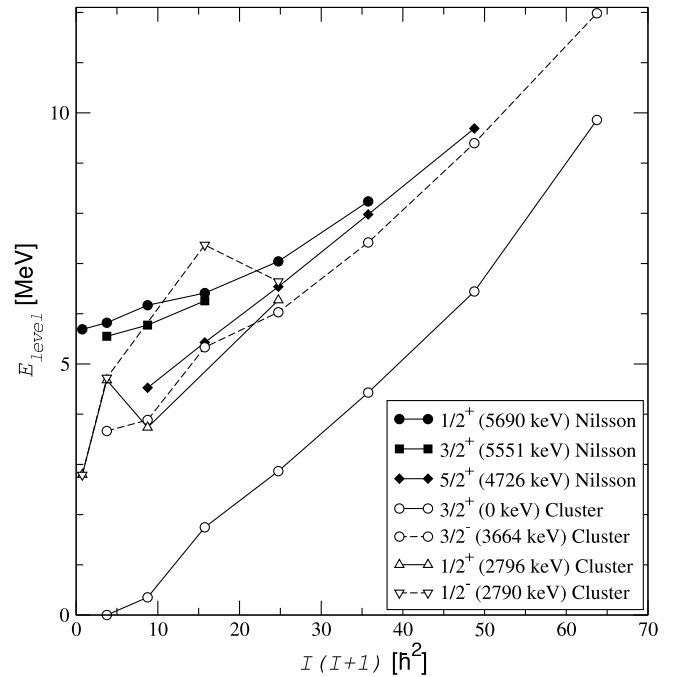


**Fig. 3.** A plot of spin ( $I(I+1)$ ) versus excitation energy for rotational bands in  $^{21}\text{Ne}$ . The close correspondence between the  $K = \frac{3}{2}$  cluster bands is evident.

the levels in each of the negative-parity bands is similar to that in the corresponding positive-parity partner, implying the same moments of inertia,  $\mathfrak{I}$ , a necessary condition for the interpretation of the bands as cluster structures. Indeed, fitting the slopes of the spin versus energy plots for the cluster bands yields  $A (= \frac{\hbar^2}{2\mathfrak{I}})$ : 0.161(8) ( $K^\pi = \frac{3}{2}^+$ )

and  $0.138(6) \text{ MeV}/\hbar^2$  ( $K^\pi = \frac{3}{2}^-$ ). For the  $K^\pi = \frac{1}{2}^+$  and  $\frac{1}{2}^-$  bands, the parameters  $A = 0.212(9)$  and  $0.201(9) \text{ MeV}/\hbar^2$  are obtained, respectively, from fitting the expression  $E = E_0 + A[I(I+1) + C(I+\frac{1}{2})(-1)^{(I+\frac{1}{2})}]$  that takes the Coriolis decoupling [19] into account. The latter two values differ from those quoted in ref. [3], due to the re-arrangement of the levels following the observation of in-band transitions in the current work and more precise level energies. While for each pair of bands the moments of inertia agree to within two standard deviations, the difference between the two values for the  $K = \frac{3}{2}$  doublet is expected, since at higher excitation energies the clusters are expected to be better formed and hence more separated, *i.e. the nucleus is more deformed*.

In the  $K = \frac{3}{2}$  cluster bands, the energy splitting, which is related to the tunnelling probability between one orientation and its reflection (*i.e.* of the  $\alpha/{}^5\text{He}$  through the  ${}^{17}\text{O}/{}^{16}\text{O}$ ), is large, 3664 keV, suggesting a sizeable tunnelling probability. For the  $K = \frac{1}{2}$  arrangement the energy splitting is negligible implying no significant tunnelling. This effect can be described by the occupation of different orbitals by the “covalent” neutron. When the neutron distribution is concentrated away from the nuclear symmetry axis in a  $\pi$ -type bond, tunnelling is permitted. The occupation of a  $\sigma$ -type bond moves the distribution on to the deformation axis, blocking tunnelling. The relevant orbital distributions are given and discussed in ref. [3]. Furthermore, the splitting between the  $K = \frac{3}{2}$  bands, though sizeable, is reduced compared to the corresponding bands in  ${}^{20}\text{Ne}$  ( $\sim 5.5 \text{ MeV}$  [3, 11]), presumably due to the reduction in tunnelling probability caused by the presence of the covalent neutron in  ${}^{21}\text{Ne}$ .

A further result from this investigation is the observation of both in-band  $E2$  transitions and out-of-band  $E1$  transitions from the same level. This enables the extraction of the electric dipole moment. Using the expressions from the rotational model [19]:

$$\begin{aligned} B(E2; I_i \rightarrow I_f) &= \frac{1}{1.225 \times 10^9 E_\gamma^5} T(E2; I_i \rightarrow I_f), \\ B(E1; I_i \rightarrow I_f) &= \frac{1}{1.59 \times 10^{15} E_\gamma^3} T(E1; I_i \rightarrow I_f), \end{aligned} \quad (1)$$

where  $T(E2)$  and  $T(E1)$  are the measured  $\gamma$ -ray transition rates and

$$\begin{aligned} B(E2; I_i K \rightarrow I_f K) &= \frac{5}{16\pi} e^2 Q_0^2 |\langle I_i 2K0 | I_f K \rangle|^2, \\ B(E1; I_i K \rightarrow I_f K) &= \frac{3}{4\pi} e^2 D_0^2 |\langle I_i 1K0 | I_f K \rangle|^2, \end{aligned} \quad (2)$$

are the reduced transition probabilities for stretched  $E2$  and stretched  $E1$  transitions, respectively. The Clebsch-Gordon coefficients [20] are:

$$\begin{aligned} |\langle I_i 2K0 | I_f K \rangle|^2 &= \left[ \frac{3(I-K)(I-K-1)(I+K)(I+K-1)}{(2I-2)(2I-1)I(2I+1)} \right] \text{ and} \\ |\langle I_i 1K0 | I_f K \rangle|^2 &= \left[ \frac{(I-K)(I+K)}{I(2I+1)} \right]. \end{aligned}$$

Taking the quotient of eqs. (1) gives the following expression:

$$\begin{aligned} \frac{D_0^2}{Q_0^2} &= 0.321016 \times 10^{-6} \frac{(E_\gamma^{E2})^5 T_1(E1)}{(E_\gamma^{E1})^3 T_2(E2)} \frac{I(2I+1)}{(I-K)(I+K)} \\ &\times \frac{3(I-K)(I-K-1)(I+K)(I+K-1)}{(2I-2)(2I-1)I(2I+1)}. \end{aligned} \quad (3)$$

Knowing the quadrupole moment,  $Q_0$ , enables the dipole moment,  $D_0$ , to be obtained. For the ground state of  ${}^{21}\text{Ne}$ ,  $Q_0 = 0.52(5) \text{ eb}$  [11], leading to a value of  $D_0 = 0.0337(79) \text{ e fm}$  for the 6030 keV  $I^\pi = \frac{9}{2}^-$  state. (The observed  $E1$  rate has been corrected for  $M2$  admixtures using the measured quadrupole/dipole mixing ratio,  $\delta = -0.08_{-4}^{+5}$  [11].) For this particular level, the  $\Delta I = 0$   $E1$  branch has also been observed, in addition to the stretched  $E1$  branch. Repeating the above procedure for such a case with the corresponding Clebsch-Gordon coefficient [20]:  $|\langle I_i 0K0 | I_f K \rangle|^2 = \left[ \frac{K^2}{I(I+1)} \right]$ , yields  $D_0 = 0.097(19) \text{ e fm}$  (using the measured value,  $\delta = -0.08(13)$  [11]). These two values for  $D_0$  only agree at the three-standard-deviation level, though they are both close to the previously reported limit of  $D_0 > 0.09$  [9]. (Note that in ref. [9] a limit of  $D_0 > 0.1$  was quoted, using  $Q_0 = 0.58(3) \text{ eb}$  from  ${}^{20}\text{Ne}$ .) Theoretical input enabling a comparison to this experimental result would be welcome, as the electric dipole moment must normally be evaluated on a nucleus-by-nucleus basis. However, the order of magnitude of the dipole moment is consistent with an octupole-deformed potential.

In ref. [9] extensions of the  $K = \frac{1}{2}$  cluster bands are suggested on the basis of known states, but as outlined above, the specific observation of in-band  $\gamma$ -decays can lead to a significant re-interpretation of such levels and firm band assignments. Specifically, the suggested [9] extensions are  $K^\pi = \frac{1}{2}^+$ : 7649(1) ( $\frac{7}{2}$ ), 9944(1) ( $\frac{13}{2}$ ) and 12451(2) keV ( $\frac{11}{2}$ );  $K^\pi = \frac{1}{2}^-$ : 12315(2) keV ( $\frac{11}{2}$ ) with energies from ref. [11]. Note that for the  $K^\pi = \frac{1}{2}^-$  band the predicted energy is 9860 keV for the  $\frac{13}{2}$  state [9], but this is already assigned to the ground-state band. However, several alternative candidate states are known in the energy range 9475–10542 keV [11].

In the  $K^\pi = \frac{1}{2}^-$  band the  $I = \frac{5}{2}$  member has not yet been observed and there are no suitable candidate states in the appropriate energy region. One plausible explanation for this could be a near degeneracy with the 3736 keV state in the positive-parity partner band, somewhat closer than the 6 keV separating the  $I = \frac{1}{2}$  levels. (Note that in the present work, the low intensity of the 3736 keV transition precludes a quantitative measure of such a scenario.) With thin target experiments such close-lying transitions are difficult to separate, predominantly due to the high speed of the transitions, taking place before the recoiling nucleus has stopped. Since  ${}^{21}\text{Ne}$  is stable, one possible solution would be to perform a  ${}^{21}\text{Ne}(\gamma, \gamma'){}^{21}\text{Ne}$  experiment since the  $I^\pi = \frac{5}{2}^-$  level can be excited directly via an  $E1$  transition from the ground state. However, the main

obstacle to such a measurement would be obtaining a suitable  $^{21}\text{Ne}$  target.

## 5 Summary

In summary, states up to 12 MeV, many above the particle thresholds ( $S_n = 6.761$  MeV,  $S_\alpha = 7.348$  MeV), have been populated in  $^{21}\text{Ne}$  using the incomplete-fusion reaction  $^{16}\text{O}(^7\text{Li}, np)^{21}\text{Ne}$  at 29.4 MeV. The  $\gamma$ -ray decay of the cluster bands has been elucidated up to spin  $\frac{15}{2}$ . Several levels have been re-assigned on the basis of the new  $\gamma$ -ray information and the electric dipole moment for the  $K^\pi = \frac{3}{2}^-$  band has been extracted. The level energies are discussed and in several cases more precisely determined than earlier work. Furthermore, a possible solution to the missing  $K^\pi = \frac{1}{2}^-, \frac{5}{2}$  state has been proposed.

The technical staff at LNL are thanked for providing the lithium beam. Dr Martin Freer is thanked for helpful discussions. This work is supported by the German BMBF. One of the authors, C. Wheldon, is grateful for the support of the Alexander von Humboldt Foundation.

## References

1. C.M. Jones, G.C. Phillips, Philip D. Miller, Phys. Rev. **117**, 525 (1960).
2. Yoshiko Kanada-En'yo, Hisashi Horiuchi, Akira Ono, Phys. Rev. **C 52**, 628 (1995) and references therein.
3. W. von Oertzen, Eur. Phys. J. A **11**, 403 (2001).
4. P.A. Butler, W. Nazarewicz, Rev. Mod. Phys. **68**, 394 (1996).
5. D. Bazzacco, *Proceedings of the International Conference on Nuclear Structure at High Angular Momentum*, Vol. **II**, Report No. AECL 10613 (AECL Research, Ottawa, 1992) p. 376.
6. E. Farnea *et al.*, Nucl. Instrum. Methods Phys. Res. A **400**, 87 (1997).
7. D. Bazzacco, C. Ur, *GASPPWARE* analysis suite, unpublished (1997).
8. D.C. Radford, Nucl. Instrum. Methods Phys. Res. A **361**, 297 (1995).
9. S. Thummerer *et al.*, J. Phys. G **29**, 509 (2003).
10. D.C. Radford, Nucl. Instrum. Methods Phys. Res. A **361**, 306 (1995).
11. R.B. Firestone, Nucl. Data Sheets **103**, 269 (2004); R.B. Firestone, V.S. Shirley (Editors), *Table of Isotopes*, 8th edition (John Wiley and Sons, 1996).
12. A. Hoffman, P. Betz, H. Röpke, B.H. Wildenthal, Z. Phys. A **332**, 289 (1989) and references therein.
13. J.N. Hallock, H.A. Enge, J.D. Garrett, R. Middleton, H.T. Fortune, Nucl. Phys. A **252**, 141 (1975).
14. G. Andritsopoulos, W.N. Catford, E.F. Garman, D.M. Pringle, L.K. Fifield, Nucl. Phys. A **372**, 281 (1981).
15. C. Rolfs, H.P. Trautvetter, E. Kuhlmann, F. Riess, Nucl. Phys. A **189**, 641 (1972).
16. D.C. Bailey, P.E. Carr, J.L. Durell, A.N. James, M.W. Greene, J.F. Sharpey-Schafer, J. Phys. A **4**, 908 (1971).
17. H. Grawe, F. Heidinger, K. Kandler, Z. Phys. A **280**, 271 (1977).
18. J.C. Lawson, P.R. Chagnon, Phys. Rev. C **11**, 643 (1975).
19. Aage Bohr, Ben R. Mottelson, *Nuclear Structure*, Vol. **II** (W.A. Benjamin Inc., 1975).
20. E.U. Condon, G.H. Shortley, *The Theory of Atomic Spectra* (Cambridge University Press, Cambridge, 1935, reprinted 1963) pp. 76-77.